

The spatial information preservation method: Sampling the nanoscale spatial distribution of microorganisms

Christopher Krembs

Institut für Polarökologie, Wischofstr. 1-3, Gebäude 12, D-24148 Kiel, Germany

Andrew R. Juhl¹

Marine Life Research Division, Scripps Institution of Oceanography, UCSD, La Jolla, California 92093-0208

J. Rudi Strickler

University of Wisconsin–Milwaukee, Center for Great Lakes Studies, 600 E. Greenfield Ave., Milwaukee, Wisconsin 53204

Abstract

It has been hypothesized that plankton patchiness exists on scales of tens to hundreds of micrometers (nanoscale patchiness). Current sampling methods disrupt the spatial pattern on this scale and therefore cannot detect nanoscale patchiness. We describe a method that allows the collection of microorganisms and other particles without destroying their relative spatial distribution. Our spatial information preservation (SIP) method is based on rapidly freezing a small sample of water. The three-dimensional particle distribution captured in the ice is preserved in two dimensions as a projection on a microscope slide. Experiments were conducted on the extent of particle movement during freezing and removal of ice from around the particles, as well as the potential for cell loss during these procedures. The experiments demonstrate that microorganisms can be collected quantitatively with sufficient preservation of their spatial distribution to resolve nanoscale patchiness.

For several decades, the suggestion has been raised in the literature that planktonic microorganisms might be found in aggregations around individual phytoplankton cells or other organic particles taking advantage of dissolved organic matter diffusing from the particle (Bell and Mitchell 1972; Azam and Ammerman 1984; Bowen et al. 1993). Such aggregations would result in patchiness of planktonic microorganisms on the scale of tens to hundreds of micrometers. We extend the nomenclature of Haury et al. (1978) by calling this nanoscale patchiness.

Patchiness can only be detected if the scale of sampling matches the scale of aggregation (Wiens 1989). However, most commonly used oceanographic methods collect samples that are orders of magnitude too large to detect nanoscale patches (Duarte and Vaqué 1992). A recent study by Müller-Niklas et al. (1996) approached the question of nanoscale patchiness by examining the variance in bacterial counts between replicate subsamples of ~100 nl. Their findings did not support the existence of nanoscale patchiness.

However, as pointed out by the authors, their sampling method, as with most typically used oceanographic methods, could have destroyed any aggregations of bacteria that were present, leaving the existence of nanoscale patches an open question. We herein outline a new method, the spatial information preservation (SIP) method, that can be used to quantitatively collect small samples of microorganisms while preserving the spatial distribution of the organisms and other particles relative to one another.

The SIP method can be separated into several procedures. We have conducted experiments to determine the degree to which information about the spatial distribution of particles is maintained for each step of the method. Our goal is to demonstrate that the SIP method preserves sufficient information about the relative spatial distribution of particles present in a water sample to assess whether aquatic microorganisms are found in nanoscale patches.

Materials and methods

Description of the SIP method—The first step of the SIP method is freezing a sample out of the water column. Once incorporated into ice, particles can no longer move. The sampling device used in our experiments (Fig. 1) consisted of a metal membrane that was exposed to the water on one surface and could be rapidly cooled from the opposite side. We constructed our membrane of fine silver (99% pure) because of its excellent heat conductivity and resistance to corrosion. The membrane was 350 μm thick, and the area exposed to the water was 0.5×1.0 cm. The cryogen used was liquid propane precooled to approximately -196°C with liquid N_2 (Silvester et al. 1982; Bald 1985). Fins mounted on

¹Corresponding author.

Acknowledgments

The authors gratefully acknowledge I. Galvan, L. Small, L. Fesenden, G. Taghon, B. Sherr, E. Sherr, and F. Azam for their help and encouragement. Portions of this work were conducted at the College of Oceanic and Atmospheric Sciences, Oregon State University; the Center for Great Lakes Studies, University of Wisconsin–Milwaukee; the Institut für Polarökologie and the Institut für Meereskunde, Christian-Albrechts Universität, Kiel; and Scripps Institution of Oceanography, University of California–San Diego. Reviews by D. Kirchman and three anonymous reviewers improved an earlier version of this manuscript.

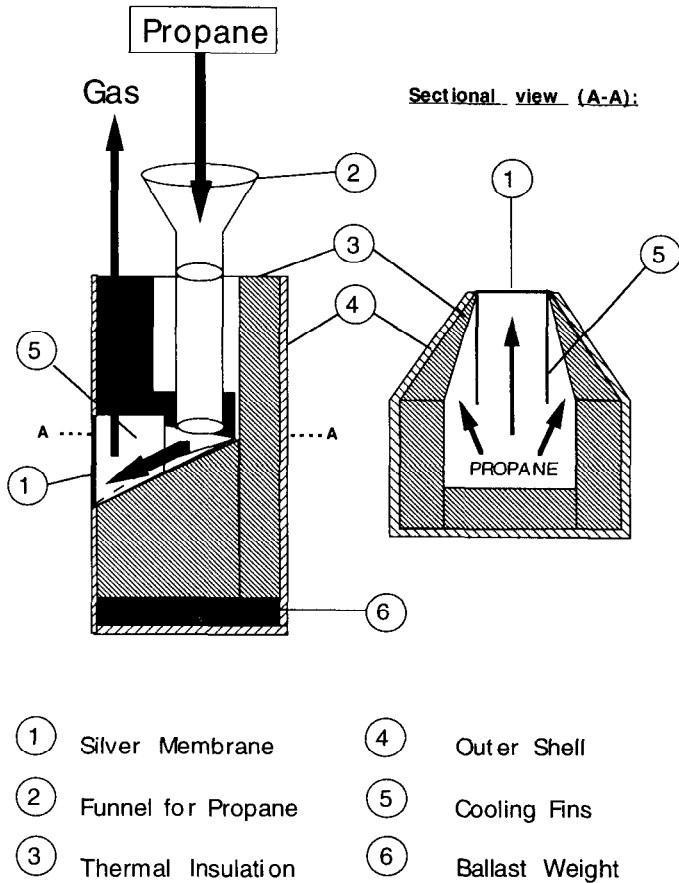


Fig. 1. Sketch of a sampler designed for laboratory experiments. Sectional view illustrates path of cryoagent when poured into the sampler.

the inner surface of the membrane decreased the ratio of membrane area exposed to water vs. the area exposed to cryogen to 0.06. We used a vertically oriented freezing membrane because preliminary video observations (*see below*) had shown that a horizontal membrane froze water more slowly. In the video viewings we also observed particles settling due to gravity onto the horizontal membrane prior to freezing.

In our experiments, the sampler was immersed in a tank. Sufficient time was allowed for water motion to cease (5–10 min). Freezing of a sample was initiated by manually pouring the cryogen into the sampler (Fig. 1). Freezing was terminated by pulling the entire sampler out of the tank. The ice (1–2 mm thick) was gently pried off the metal membrane and stored in liquid N_2 . The ice was kept below $-20^\circ C$ to prevent recrystallization (Bari and Hallett 1974).

The next objective was to remove the ice from around the organisms without distorting their spatial orientation relative to one another. We accomplished this during the ice substitution procedure, which is similar to the filter-transfer-freeze method (Hewes and Holm-Hansen 1983). Ice-substitution techniques have been used in electron microscopy (e.g. Steinbrecht and Müller 1987).

A glycerol-gel mixture (16% Knox gelatin, 30% Sigma-grade glycerol, 54% water, wt/vol) was made. The mixture

was heated to dissolve the gelatin. Wire loops (~ 2 cm in diam) were dipped into the gel while it was still liquid. This produced a thin film of glycerol-gel suspended within the wire loop. The loops were allowed to solidify at $-15^\circ C$.

The frozen sample was placed on the suspended glycerol gel film. To prevent the ice from melting, while simultaneously allowing for a reasonably rapid substitution, the temperature was maintained at $-15^\circ C$ inside an insulated box that was connected by two pipes to a large freezer. A small fan installed inside the freezer produced a circulation from the freezer to the insulated box and then back to the freezer through the second pipe. Water vapor in the return flow from the box settled out as frost due to the colder temperature inside the freezer, thus maintaining very low humidity inside the box. A plastic cup was placed over the loop to prevent the exposed surface of the ice from sublimating. During ~ 24 –72 h, the ice slowly dissolved into the glycerol gel. The water molecules migrated into the gel due to the hygroscopic properties of the glycerol. Water was constantly removed from the underside of the gel by the flow of cold, dry air. This prevented the build up of water and thereby prevented particle movement. As the ice dissolved, the organisms that had been frozen in the ice matrix adhered to the surface of the gel. Once the desired thickness of ice had been substituted onto the gel, the remaining ice was peeled off with cold forceps. During the next 6 h, the temperature was gradually raised to $4^\circ C$. Very low humidity was maintained during this entire process by loading the box with Drierite.

A glass microscope slide was coated with a film of glycerol. The wire loop, with its suspended glycerol gel, was laid on the slide, organism side up. The gel was cut free of the loop and the slide was stored at $4^\circ C$ for 19 h in order to let the gel dry completely. A coverslip was cooled to $4^\circ C$. One drop of a glycerol/glutaraldehyde/4',6-diamidino-2-phenylindole (DAPI) (Porter and Feig 1980) solution (4.6 ml 100% Sigma-grade glycerol, 0.4 ml 25% glutaraldehyde, and 0.05 ml of a $50 \mu g ml^{-1}$ DAPI solution, $4^\circ C$) was placed on the coverslip. The coverslip was carefully laid on top of the gel, simultaneously preserving and staining the organisms. The sample was now ready for standard epifluorescence or transmitted light microscopic analysis. Experiments and observations were conducted at each of the major steps in the method described above to confirm that the SIP method preserved the spatial information that was originally present in the water column.

Video observations of the freezing process—To quantify the potential distortion of spatial information during freezing, we videotaped the freezing process at high magnification. We were able to follow the trajectories of individual organisms from before the cryogen was poured into the sampler until after they had been frozen into the ice.

The freezing process was continuously documented on videotape using a modified Schlieren optical pathway (Strickler 1977) at $250\times$ magnification with a resolution of $>10 \mu m$. The axis of the optical pathway was parallel to the silver membrane, allowing the observation of particle movement near the membrane and the buildup of ice. The light source was a high-pressure Xenon arc lamp. While the field-

to-field resolution was 16.7 ms, we found it sufficient to use full frames at intervals of 33.3 ms.

The positions of particles larger than 10 μm , the ice-water interface, and the freezing membrane within the observation area of 1.75×1.25 mm was determined using video-image analysis software (Image-Pro, Media Cybernetics). A Schlieren optical pathway allows for the observation of differences in optical density. We could therefore visualize particles, the ice, and the density gradient that formed in front of the membrane during freezing.

The sampler was immersed in the middle of a $10 \times 10 \times 15$ -cm (length \times width \times height) tank. The tank was filled with 1 liter of water from mixed cultures of either fresh- or saltwater organisms; the water temperature was always 21°C . The organisms were alive, which could be seen from the motility of some of the cells. When water motion could no longer be detected on the video monitor, 30 ml of precooled liquid propane was poured into the sampler to initiate the freezing process.

An additional series of experiments was conducted to measure the impact of salinity on the growth rate of ice. A similar optical pathway was used as in the experiments above. The light source was a HeNe laser set at 632 nm. A series of solutions with 0, 10, 20, 30, 40, and 50 g of artificial sea salt (Instant Ocean) per liter was used. The freezing rate was calculated from measurements of ice thickness on successive videoframes.

Gas bubble formation during freezing—During freezing, dissolved gases are exsolved from ice, forming a diffusion boundary layer of water supersaturated with gas, immediately in front of the advancing ice sheet (Bari and Hallett 1974). Bubbles that form in this layer are incorporated into the advancing ice and may distort the spatial distribution of particles. To quantify the size and concentration of bubbles in the ice layer, ice samples were frozen using distilled water that had been equilibrated with the overlying air at 21°C . The same sampling device was used as in the video experiments above. A 500-ml tank was used. After freezing, the ice was pried off the sampler membrane and stored in liquid nitrogen for 1 week.

In order to cut the ice into small pieces, the ice was removed from the liquid nitrogen and immediately placed onto a small piece of damp wood that had been cooled to just below 0°C . The ice froze instantly to the wood and could be cut into ~ 1 -mm-thick slices with a razor blade. Ice slices were examined in a -43°C room with a Zeiss light microscope at $500\times$ magnification. Concentration was estimated from 180×30 - μm transect counts at distances of 90, 270, 450, 630, 810, 990, 1,170, and 1,350 μm from the freezing membrane. The focal plane was ~ 5 μm thick, giving a volume of 27,000 μm^3 per transect.

Preservation of spatial information during the ice substitution procedure—To test whether spatial information contained in the ice was preserved during the ice-substitution procedure, it was necessary to create an easily recognizable pattern in a piece of ice. Distortion of the pattern that occurred during the ice-substitution procedure would then be apparent on the surface of the glycerol gel. We used 1.9-

μm -diameter fluorescent polystyrene beads to create a straight-line pattern in a piece of ice. A concentrated solution of beads in distilled water was poured out onto a smooth metal surface and then frozen by rapidly cooling the metal with liquid N_2 . The ice was removed from the surface and then fractured into small ($\sim 5 \times 5$ mm) pieces. The fractures produced extremely sharp edges that were approximately straight for hundreds of micrometers. The ice fragments were placed back on the cold metal surface before they could melt. Distilled water that had been cooled to 0°C was poured around the ice fragment and frozen immediately into place. The ice containing the fragment was removed from the surface and was run through the ice-substitution procedure described above. Once the ice had dissolved, the glycerol gel was mounted on a microscope slide and examined with an epifluorescence microscope ($450\times$ magnification) to see if the sharp edge in the bead pattern had been maintained.

A circular pattern of polystyrene beads was produced in ice by entrapping air bubbles. A block of aluminum was chilled with dry ice. Blowing across the surface of the block generated a layer of frost on its surface that served to trap pockets of air. A drop of a concentrated solution of 1- μm -diameter beads in distilled water was pipetted onto the surface of the block. The bead solution melted the frost, but then froze, entrapping hemispherical air bubbles at the ice-metal interface. The ice was then peeled off the surface of the block and transferred to a glycerol gel (with the formerly metal-facing surface down) for the ice substitution procedure. Ice substitution was terminated by removing the ice sample after the first few tens of microns of ice had been substituted. The gel was mounted on a slide and microscopically inspected as described for the other pattern above.

Quantitative comparison of the freezing process and ice-substitution procedure to the standard filtration method—Because cell loss might occur during the freezing process and ice-substitution procedure, we tested the effect of these procedures on quantitative cell counts in isolation from the rest of the SIP method. For comparison, cell abundance was measured with the standard filtration method (e.g. Hobbie et al. 1977). Water with a natural assemblage of plankton was collected from Lake Kleiner Kiel (Kiel, Germany). Fluorescent microbeads (1.9 μm in diam) were added to the water at a concentration of $\sim 5,000$ beads ml^{-1} as an internal reference for pipetting errors. Control slides were made from 200- μl subsamples. Subsamples were diluted in 5 ml of 0.2- μm filtered lake water in order to ensure that particles would be evenly distributed when filtered. The samples were fixed with ice-cold glutaraldehyde (final concn of 2%), stained with DAPI (4 $\mu\text{g ml}^{-1}$; Porter and Feig 1980) for 5 min and then filtered onto black 0.2- μm Nuclepore polycarbonate membrane filters with a 20- μm glass-fiber backing filter at 0.175 bar vacuum pressure.

Parallel 200- μl treatment subsamples were also taken. These subsamples were frozen on a horizontal copper membrane with liquid N_2 as the cryoagent. These frozen droplets were maintained in small aluminum trays at -20°C . Two hundred microliters of Sigma-grade glycerol was added to each droplet. After 24 h, the ice had dissolved and the samples were diluted with 5 ml of filtered lake water. The sam-

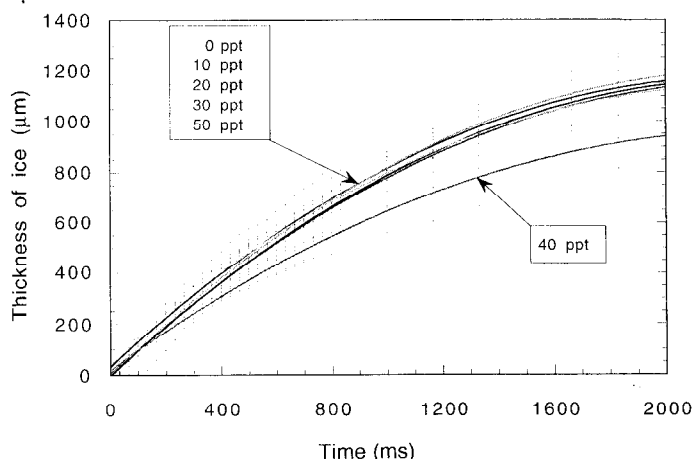


Fig. 2. Impact of salinity on the growth of ice. The graph shows ice thickness over time for salinities from 0 to 50 ppt. Three trials were run for each salinity. The curves are polynomial regression lines; $r^2 > 0.96$ in each case. The initial delay in freezing is not readily apparent due to the x -axis scale.

ples were fixed, stained, and filtered in the same way as the control samples above.

Three replicate filters were counted in each case. All filters were counted with a Zeiss Axioplan epifluorescence microscope equipped with blue light (450–490 nm) and UV (365 nm) excitation filter sets.

Results

The ice samples collected were uniform in thickness and consisted of “pure ice” (*sensu* Nishimura et al. 1991). Dendritic ice crystal formation was not observed. The freezing rate was continuously determined as the ice grew (Fig. 2). The freezing rate decreased with time as the ice grew thicker. We observed a delay between initial membrane cooling and the beginning of ice formation. This delay lasted 100 ms in freshwater and ~255 ms in seawater.

Observations of particles during the freezing process revealed that a downward-directed density current formed in front of the advancing ice layer due to the cooling of water immediately in front of the ice. As would be predicted from the size scale of the observations and the consequent low Reynolds number, the flow was laminar. The observed flow was always directed downward. Density-inversion currents (Tankin and Farhadie 1971; Nishimura et al. 1990, 1991) were not seen. As the ice grew into the water column, particles in front of the ice were displaced downward before being frozen into the ice matrix. As particles entered the density flow, they accelerated to a maximum velocity near the middle of the current and then, as the ice grew closer, they decelerated back to zero before freezing into the ice. The maximum downward velocity increased with time. In seawater, the maximum velocity was higher than in freshwater. The apparent width of the current also increased over time and was always greater in seawater than in freshwater.

Because the freezing rate decreased with time while the width and maximum velocity of the density current increased with time, particles had greater downward displace-

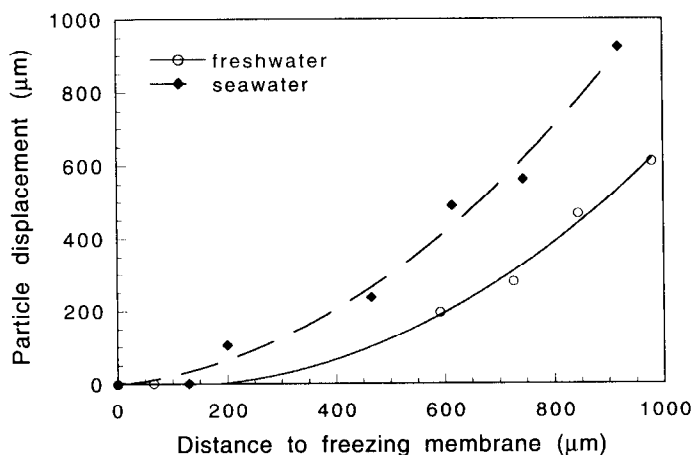


Fig. 3. Absolute downward displacement of particles due to the density current vs. their initial distance to the membrane.

ment before being incorporated into the ice the farther they were away from the metal membrane (Fig. 3). The displacement was greater in seawater than in freshwater. Table 1 summarizes the observed differences in the freezing of freshwater and seawater.

Although the smallest particles that were observed on video were ~10 µm across, bacteria-sized particles (generally ≤ 1 µm in diam) should have behaved similarly, since the current was laminar. Particle movement was strictly linear and directed downward; no horizontal movement (perpendicular to the flow) could be observed. This is expected in a laminar-flow field with a sufficiently small particle Reynolds number (Ho and Leal 1974). Importantly, the particles that we observed were live organisms, and even motile forms were captured effectively. Motile organisms behaved as passive particles once they entered the density current. Presumably, the cold temperature induced a thermal shock after which they could no longer swim significantly. Particles were often still visible once they froze into the ice. No movement could be detected once they were frozen.

Table 1. Summary of observed differences between seawater and freshwater during vertical freezing at an initial water temperature of 21°C.

Character	
Growth of ice	Growth rate decreased over time; was similar for all salinities except 40 ppt
Delay in onset of ice formation after membrane cooling began	Delay was longer in seawater
Width of density current	The width increased over time; current was wider in seawater
Max. velocity of density current	The velocity increased over time; was always higher in seawater
Particle displacement	Displacement increased with distance from membrane; was greater in seawater

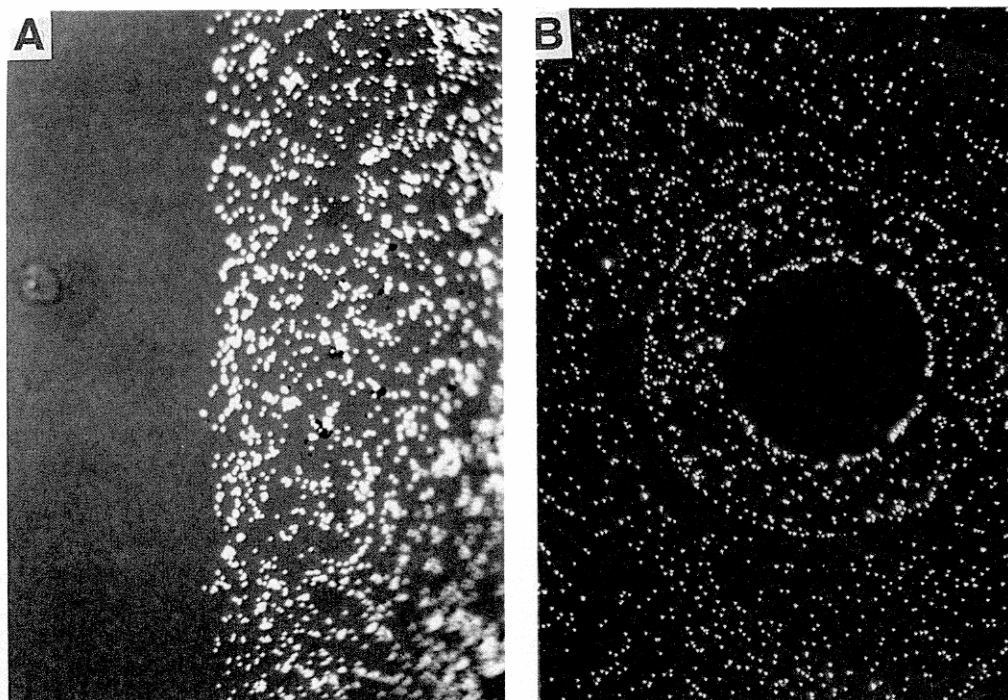


Fig. 4. A. Photomicrograph of the edge of a straight-line bead pattern. The beads average $1.9 \mu\text{m}$ in diameter. The dark spots are dust particles that settled on the gel surface because these samples were not covered following ice substitution. B. Photomicrograph of a circular void in the field of beads generated by a partially substituted air bubble. The beads average $1 \mu\text{m}$ in diameter.

In our first test of the ice-substitution procedure, we assumed that if no movement of the beads had occurred we would see a distinct straight-line pattern on the gel. In each of the 10 trials a sharp edge was clearly seen. A sample photomicrograph from the trials is shown in Fig. 4A. We are confident that we would have detected random movements of the beads on the order of $5\text{--}10 \mu\text{m}$ because the edge that the beads described was so sharp. In the second test we expected to find circular voids in the field of beads where the hemispherical bubbles at the ice-metal interface had been. An example of such a circular void is shown in Fig. 4B. Again, the pattern in the ice was not obscured during

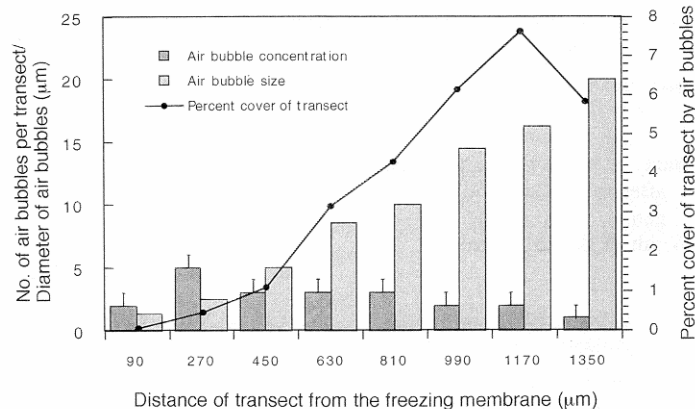


Fig. 5. Number and size of air bubbles per transect vs. distance from the transect to the freezing membrane. Also shown is the percent areal cover by bubbles in each transect.

ice substitution. This second test was undertaken exclusively to demonstrate the effectiveness of the ice-substitution procedure and should not be confused with the bubbles that form at the ice-water interface during freezing out of a water column. The bubbles of the ice-substitution test were generated on purpose at the metal interface and were comparatively large in diameter. Because the freezing rate during the test was slow, and because the ice was frozen in a horizontal orientation, the particle distribution outside the bubble would have been distorted during freezing.

The size and concentration of bubbles formed at the ice-water interface by the exsolution of gases during freezing were determined along microscopic transects within the ice. Within each transect, bubbles appeared randomly distributed. The bubbles appeared spherical in all transects excepting the one farthest from the freezing membrane (at $1,350 \mu\text{m}$ from the membrane), where the bubbles appeared ovoid. The diameter of the bubbles increased with increasing distance from the freezing membrane (Fig. 5). Concentration ranged from $3.7\text{--}18.5 \times 10^7 \text{ ml}^{-1}$, with the maximum being between 180 and $360 \mu\text{m}$ from the freezing membrane (Fig. 5). The percent areal cover at the ice-water interface was calculated from mean diameter and concentration of bubbles for each transect. Percent cover increased with increased distance from the membrane (Fig. 5).

Table 2 shows the comparison between counts of bacteria, autotrophic flagellates, fluorescent beads, and two species of nonflagellated algal cells, for samples that were preserved and then filtered, vs. samples that were first frozen, then dissolved in glycerol and then filtered. Freezing followed by

Table 2. Comparison between counts of fluorescent beads and organisms in unmanipulated samples (control) vs. samples that were frozen and dissolved in glycerol (treatment). Values are means of three replicates; standard deviations are in parentheses. Bacteria were enumerated in 20 random fields per filter at 1,000 \times magnification. Nonflagellated algal cells (*Kirchneriella obesa* and *Crucigenia rectangularis*) and fluorescent beads were counted in 155 fields per filter at 650 \times magnification. No significant differences were observed between control and treatment samples (two-tailed *t*-test, $P > 0.2$ for each comparison, 4 df).

Category	No. ml ⁻¹	
	Control	Treatment
Fluorescent beads	3.5 \times 10 ⁴ (0.7 \times 10 ⁴)	3.4 \times 10 ⁴ (0.1 \times 10 ⁴)
Autotrophic flagellates	1.2 \times 10 ⁴ (0.3 \times 10 ⁴)	1.5 \times 10 ⁴ (0.6 \times 10 ⁴)
Bacteria	5.7 \times 10 ⁷ (1.0 \times 10 ⁷)	5.1 \times 10 ⁷ (0.1 \times 10 ⁷)
<i>K. obesa</i>	8.3 \times 10 ³ (1.5 \times 10 ³)	7.0 \times 10 ³ (2.6 \times 10 ³)
<i>C. rectangularis</i>	4.0 \times 10 ³ (1.7 \times 10 ³)	4.0 \times 10 ³ (2.0 \times 10 ³)

dissolution in glycerol did not have a significant effect on the counts.

Discussion

We have conducted experiments to quantify the degree to which the in situ spatial pattern is distorted along each step of the SIP method. Our conclusion is that the error introduced using the SIP method will not obscure the signal of nanoscale plankton patchiness. The largest source of error is caused by the downward displacement of particles in the density current immediately in front of the growing ice. However, for preserving spatial information, the absolute downward displacement of single particles before becoming frozen into the ice is not directly relevant—it is the relative displacement between particles that must be considered. The relative particle displacement is determined by the differences between the absolute displacements of particles and is therefore much smaller. Relative displacement of particles depends only on the initial distance between particles per-

pendicular to the density flow and the distance from the particles to the freezing membrane. Fig. 6A shows the final relative downward displacement that would be preserved in the ice for particles separated by initial horizontal distances of 10, 100, and 300 μ m in freshwater (21 $^{\circ}$ C). Fig. 6B shows the same result for seawater. Because organisms in a patch would be separated from each other and from the freezing membrane by different distances, and because the density current would cause unidirectional “stretching” of any such patch, a hypothetically spherical patch of microorganisms would end up being distorted into an ovoid shape in the ice since those portions of the patch farthest from the membrane have the greatest displacement. The distortion would increase with larger patch diameter and greater initial patch-to-freezing membrane distance.

Data on freezing rate and absolute and relative particle displacement are given for an initial water temperature of 21 $^{\circ}$ C since this was the water temperature for experiments described here and in the accompanying paper (Krembs et al. 1998). However, we have found that both absolute and relative particle displacement are substantially decreased at lower initial water temperatures (Krembs 1996). The characteristics of the density current can be expected to change depending on initial water temperature (Brewster and Gebhart 1988); it is therefore necessary to monitor the freezing process for each sample collected.

The ice-substitution procedure—The objective of the ice-substitution procedure is to separate the organisms from the ice so that they can be viewed without destroying their relative spatial distribution. Two artificially created patterns of polystyrene beads survived the procedure without significant bead movement. Assuming that organisms behave in the same way, the ice substitution procedure will not destroy naturally occurring nanoscale patterns in organism distribution.

The major consequence of the ice-substitution procedure is that the three-dimensional particle distribution in the ice is reduced to two dimensions on the surface of the glycerol

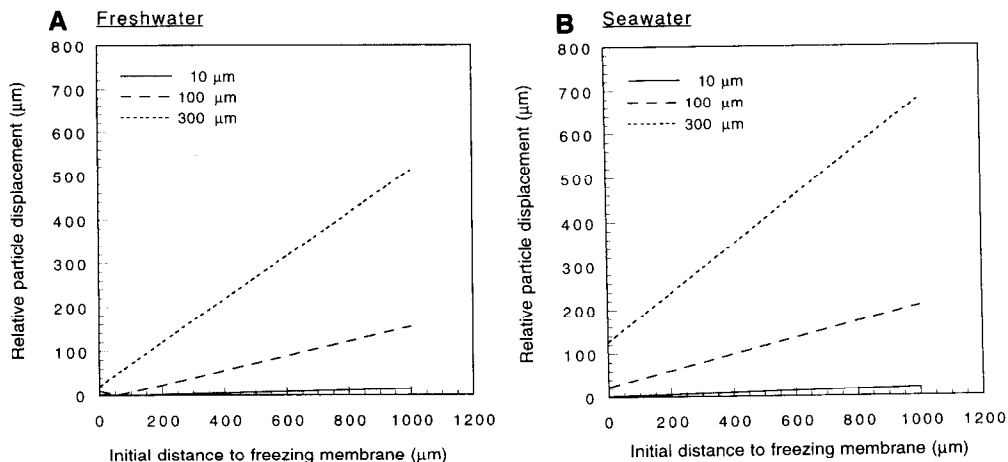


Fig. 6. Relative displacement during the freezing process by two particles initially separated by 10, 100, and 300 μ m on a line perpendicular to the density current flow depending on the initial distance from the freezing membrane to the closest particle. A. Freshwater. B. Seawater.

Table 3. Calculated probability (assuming a Poisson distribution) of sampling a single quadrat with the given number of cells after substituting 100 or 1,000 μm of ice.

Cells quadrat ⁻¹	Probability	Expected frequency*
100 μm of ice†		
0	0.99	990,050
1	0.0099	9,900
2	4.95×10^{-5}	50
3	1.65×10^{-7}	<1
1,000 μm of ice‡		
0	0.905	904,837
1	0.090	90,484
2	0.005	4,524
3	0.0001	151
4	3.78×10^{-6}	4
5	7.58×10^{-8}	<1

* No. occurrences out of 10^6 total quadrats.

† Total of 10^4 bacteria on the gel surface; expected mean of 0.01 bacteria quadrat⁻¹.

‡ Total of 10^5 bacteria on the gel surface; expected mean of 0.1 bacteria quadrat⁻¹.

gel. As a consequence of this compression, some information about the spatial distribution of particles will be lost, since particles that were initially separated horizontally can end up next to each other. However, it is unlikely that false "patches" would be formed during the substitution procedure owing to the low density of bacteria in natural water samples, meaning that cells that are not members of a single patch are widely spaced from each other. Thus, the probability that two or more cells (not of a single patch) would end up near each other on the gel surface is very low, even following compression of the three-dimensional distribution onto a plane.

The probability of finding any selected cell concentration within quadrats of a given size on the surface of the gel can be calculated for the null model of randomly distributed cells (i.e. Poisson distribution) given the thickness of ice substituted, the cell concentration within the ice, and the area and number of quadrats sampled. Assume an ice piece that is $1 \times 1 \times 1$ cm (1 ml) frozen out of water with a bacterial cell concentration of 10^6 cells ml^{-1} . For each 1- μm thickness of ice substituted, one expects 100 bacteria to be deposited on the surface of the gel. We typically substitute 100–1,000 μm of ice, so we would expect 10^4 – 10^5 cells on the $10,000 \times 10,000$ - μm gel surface. If we divide the gel surface into 10×10 - μm quadrats for observation and enumeration, there are 10^6 quadrats total. The probabilities of finding a quadrat with 0–5 cells for both 100 and 1,000 μm of substituted ice are given in Table 3. Even in the extreme case of 1,000 μm of ice substituted, after examining an area as large as $1,000 \times 1,000$ μm (10,000 quadrats), one would be surprised to find as few as 4 cells in a 100 - μm^2 area ($p = 1 - (1 - 3.78 \times 10^{-6})^{10,000} = 0.04$), and one would probably reject the null hypothesis that the cells were randomly distributed. This example demonstrates the extent to which a patch can be expected to stick out on the gel surface relative to the background. Even in the extreme case of 1,000 μm of ice

substituted, >90% of the quadrats on the gel surface are expected to be empty. The background is expected to consist predominantly of widely spaced, single cells. Given such low background noise, reducing the three-dimensional distribution of bacterioplankton down to a two-dimensional pattern on the gel surface may actually make potential patches more apparent. Compressing all the cells of a patch onto a plane will raise the areal concentration to levels that are unlikely to have occurred by chance.

In addition to concentrating cells, the ice-substitution procedure is necessary to allow visualization of particles. Unstained biological particles have been observed in solid ice using TEM (Adrian et al. 1984; Stewart and Vigers 1986). However, the ice must be vitreous and very thin (no more than several hundred nanometers). The ice-substitution procedure allows the collection of ice that is sufficiently thick that it could contain entire nanoscale patches. Following ice substitution, the cells are exposed on the gel surface and can be stained using traditional techniques and are also available for other analyses.

The rate of ice substitution can be used to determine the thickness of ice substituted for any given sample. Importantly, the substitution rate depends on the air humidity, gel composition, and temperature; these factors are also critical in determining whether organisms will be lost when the ice is peeled off the gel to terminate substitution (Krembs 1996).

Gas bubble formation during freezing—Gas bubbles that form at the ice–water interface during freezing get incorporated into the ice. If these bubbles grew large enough they could disrupt the spatial distribution of particles. Bubble diameter and concentration are directly linked to freezing rate after a steady state has been reached at the ice–water interface (Bari and Hallett 1974). As freezing rate decreases, bubble concentration decreases while bubble diameter increases (Fig. 5). Because our measured freezing rates were not affected by salinity (Fig. 2), the maximum expected bubble diameter will be the same in freshwater or saltwater and will depend only on the thickness of ice substituted. Our observations demonstrate the minor effect bubbles will have on the preservation of spatial pattern (Fig. 5). Although bubbles are numerous, reaching concentrations higher than typical bacterial cell concentration, each bubble is small (<10 μm in diam for the ice thickness we typically substitute), and bubbles are widely spaced within the volume of the ice (<5 encountered along a 180×30 - μm transect). Consequently, bubbles are unlikely to displace the even more widely spaced bacterial cells. Should a bubble form near a bacterial cell, the cell will be displaced by no more than one bubble diameter. If a bubble formed within a hypothetical patch, a void could be formed within that patch. However, unless the patch were less than 10 μm in diameter, one would still see a patch, albeit distorted, on the gel surface. In summary, the error that is potentially introduced by the formation of bubbles is similar to the maximum distortion that can be expected from the ice-substitution procedure.

Comparison of the freezing process and ice-substitution procedures to the standard filtration method—The freezing and ice-substitution procedures do not bias counts of micro-

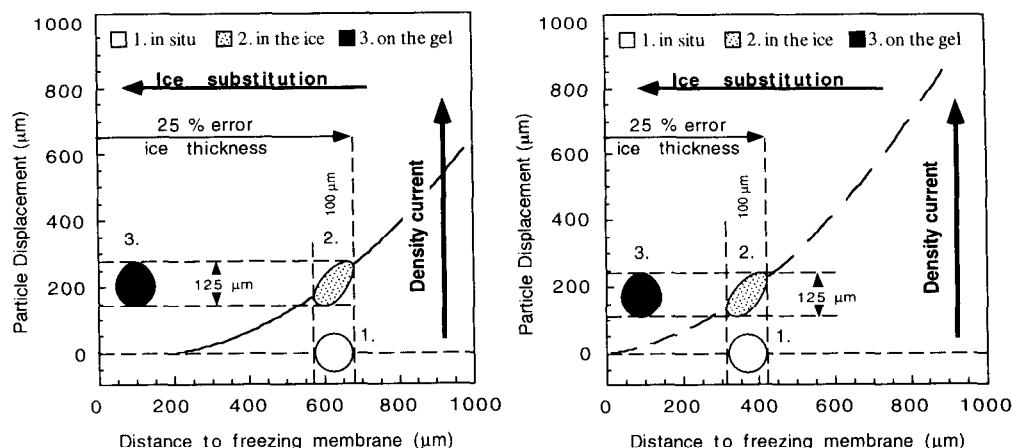


Fig. 7. A hypothetically spherical, 100- μm -diameter patch of bacteria is followed through the entire SIP method to demonstrate the distortion that occurs at the different stages of the method. A. Freshwater. B. Seawater. 1, Patch in situ—the outer edge of the patch is at a distance from the freezing membrane that will produce a final 25% stretching of the entire patch. This distance is smaller in seawater than in freshwater. 2, Patch frozen into the ice—the patch has been distorted by the particle-displacement function from Fig. 3 (shown). 3, Patch shown as it would appear on the surface of the gel. It is lengthened by 25% along the y-axis; however, the width has not increased. The z-axis has been compressed into the x-y plane. The originally spherical patch appears as a two-dimensional ovoid.

organisms relative to the standard filtration method. These results should come as no surprise because of the similarity of our method to the filter-transfer-freeze method which has been extensively tested by Hewes et al. (1984). When samples are taken through the entire ice-substitution procedure, the resulting slides are of comparable quality to slides made using the filtration method. Examples of photomicrographs of SIP slides are shown in Krembs et al. (1998).

Assessing and controlling error—The largest source of error in the SIP method is the unidirectional displacement of particles during freezing. The crucial factor in assessing and controlling this source of error is the thickness of ice that is substituted. Sufficient ice must be substituted to provide enough particles for analysis. Substitution should be terminated at that point since the ice nearest the membrane has the least relative particle displacement. Less relative displacement occurs in freshwater, allowing a thicker piece of ice to be substituted for a given level of error. Figure 7 illustrates a hypothetical 100- μm -diameter, spherical patch. Point 1 represents the patch in situ. If we accept a unidirectional distortion that will increase the patch diameter by no more than 25%, the patch can be located up to 675 μm from the freezing membrane in freshwater, 420 μm in seawater. Point 2 represents the patch after it has been frozen in the ice. Its shape is distorted according to the particle displacement function in Fig. 3. At point 3, the patch has been substituted onto the surface of the gel. Its shape is ovoid and it has been lengthened in one dimension by 25%. A smaller patch originally located at the same distance from the freezing membrane would be less distorted. The same size patch originally closer to the freezing membrane would also be less distorted.

In any given sample, owing to the two-dimensional com-

pression from the ice-substitution procedure, one cannot say how far any particle or patch was originally from the freezing membrane. One is limited to determining the maximum possible distortion based on the patch diameter and the maximum distance the patch could have been from the freezing membrane (the thickness of ice substituted). Of course, most patches will not be at the far edge of the ice and will therefore be less distorted. Bubble formation during freezing and particle movement during the ice-substitution procedure both produce random particle displacement of ~ 10 μm . Combining all sources of error, it is still expected that nanoscale patchiness could be resolved in samples. This is largely due to the low concentration of cells in natural, aquatic systems, leading to a very large difference in cell-cell spacing between a patchy vs. a random cell distribution.

Sufficient indirect evidence indicates that nanoscale plankton patchiness exists to make study of the phenomena worthwhile. The SIP method quantitatively samples microorganisms while sufficiently preserving their spatial orientation relative to one another to resolve potential nanoscale patchiness. Other approaches have been used to study the nanoscale distribution of bacterioplankton. Indirect evidence and modeling (Azam and Ammermann 1984; Blackburn et al. 1997; Bowen et al. 1993; Jackson 1987, 1989; Mitchell et al. 1985) are by themselves unconvincing. Replicate counts of very small samples could provide statistical evidence for patchiness (Duarte and Vaqu e 1992; M uller-Niklas et al. 1996), but only if the sampling protocol does not disrupt the patches or homogenize a volume that is large relative to the patch size. Direct microscopic observation relies on creating artificial cell concentrations and chemical gradients (Mitchell et al. 1996). The SIP method provides direct evidence regarding the nanoscale distribution of aquatic microorganisms with the additional advantage that the cells are

actually collected and available for further analyses. Use of labeled substrates, molecular probes, or in situ PCR in conjunction with the SIP method could reveal physiological information on individuals whose spatial distribution relative to particles, phytoplankton, and other cells is known. In conjunction with such techniques, the SIP method may find application to other questions where the relative spatial distribution of aquatic microorganisms is important.

References

- ADRIAN, M., J. DUBOCHET, J. LEPAULT, AND A. W. McDOWALL. 1984. Cryo-electron microscopy of viruses. *Nature* **308**: 32–36.
- AZAM, F., AND J. W. AMMERMAN. 1984. Cycling of organic matter by bacterioplankton in pelagic marine ecosystems, microenvironmental considerations, p. 345–360. *In* M. J. R. Fasham [ed.], *Flows of energy and nutrients in marine ecosystems*. Plenum.
- BALD, W. B. 1985. The relative merits of various cooling methods. *J. Microsc.* **140**: 17–40.
- BARI, S. A., AND J. HALLETT. 1974. Nucleation and growth of bubbles at an ice–water interface. *J. Glaciol.* **13**: 489–518.
- BELL, W., AND R. MITCHELL. 1972. Chemotactic and growth responses of marine bacteria to algal extracellular products. *Biol. Bull.* **143**: 265–277.
- BLACKBURN, N., AZAM, F., AND A. HAGSTRÖM. 1997. Spatially explicit simulations of a microbial food web. *Limnol. Oceanogr.* **42**: 613–622.
- BOWEN, J. D., K. D. STOLZENBACH, AND S. W. CHISHOLM. 1993. Simulating bacterial clustering around phytoplankton cells in a turbulent ocean. *Limnol. Oceanogr.* **38**: 36–51.
- BREWSTER, R. A., AND B. GEBHART. 1988. An experimental study of natural convection effects on downward freezing of pure water. *Int. J. Heat Mass Transfer* **31**: 331–348.
- DUARTE, C. M., AND D. VAQUÉ. 1992. Scale dependence of bacterioplankton patchiness. *Mar. Ecol. Prog. Ser.* **84**: 95–100.
- HAURY, L. R., J. A. MCGOWAN, AND P. H. WIEBE. 1978. Pattern and processes in time–space scales of plankton distributions, p. 277–327. *In* J. H. Steele [ed.], *Spatial patterns in plankton communities*. NATO Conferences Series IV: Marine Sciences. Plenum.
- HEWES, C. D., AND O. HOLM-HANSEN. 1983. A method for recovering nanoplankton from filters for identification with the microscope: The filter-transfer-freeze (FTF) technique. *Limnol. Oceanogr.* **28**: 389–394.
- , M. H. F. REID, AND O. HOLM-HANSEN. 1984. The quantitative analysis of nanoplankton: A study of methods. *J. Plankt. Res.* **6**: 601–613.
- HO, B. P., AND L. G. LEAL. 1974. Inertial migration of rigid spheres in two-dimensional unidirectional flow. *J. Fluid Mech.* **68**: 365–400.
- HOBBIE, J. E., R. J. DALEY, AND S. JASPER. 1977. Use of Nuclepore filters for counting bacteria by fluorescence microscopy. *Appl. Environ. Microbiol.* **33**: 1225–1228.
- JACKSON, G. A. 1987. Simulating chemosensory responses of marine microorganisms. *Limnol. Oceanogr.* **32**: 1253–1266.
- . 1989. Simulation of bacterial attraction and adhesion to falling particles in an aquatic environment. *Limnol. Oceanogr.* **34**: 514–530.
- KREMB, C. 1996. The examination of a method and its relevance to sample the distribution of aquatic microorganisms on scales of micrometers to centimeters. Ph.D. thesis, Christian-Albrechts Universität. 155 p.
- , A. R. JUHL, R. A. LONG, AND FAROOQ AZAM. 1998. Nano-scale patchiness of bacteria in lake water studied with the spatial information preservation method. *Limnol. Oceanogr.* **43**: 307–314.
- MITCHELL, J. G., A. OKUBO, AND J. A. FUHRMAN. 1985. Microzones surrounding phytoplankton form the basis for a stratified marine microbial ecosystem. *Nature* **361**: 58–59.
- , L. PEARSON, AND S. DILLON. 1996. Clustering of marine bacteria in seawater enrichments. *Appl. Environ. Microbiol.* **62**: 3716–3721.
- MÜLLER-NIKLAS, G., M. AGIS, AND G. J. HERNDL. 1996. Microscale distribution of bacterioplankton in relation to phytoplankton: Results from 100-ml samples. *Limnol. Oceanogr.* **41**: 1577–1582.
- NISHIMURA, T., M. FUJIWARA, AND H. MIYASHITA. 1990. Visualization of temperature fields of transient natural convection with maximum density effect in a water-filled enclosure by chiral nematic liquid crystals. *J. Chem. Eng. Jpn.* **23**: 241–244.
- , ———, AND ———. 1991. Temperature visualization by use of liquid crystals of unsteady natural convection during supercooling and freezing of water in an enclosure with lateral cooling. *Int. J. Heat Mass Transfer* **34**: 2663–2668.
- PORTER, K. G., AND Y. S. FEIG. 1980. The use of DAPI for identifying and counting aquatic microflora. *Limnol. Oceanogr.* **25**: 943–948.
- SILVESTER, N. R., S. MARCHESI-RAGONA, AND D. N. JOHNSTON. 1982. The relative efficiency of various fluids in rapid freezing of protozoa. *J. Microsc.* **128**: 175–186.
- STEINBRECHT, R. A., AND M. MÜLLER. 1987. Freeze-substitution and freeze drying, p. 149–174. *In* R. A. Steinbrecht and K. Ziergold [eds.], *Cryotechniques in biological electron microscopy*. Springer-Verlag.
- STEWART, P. L., AND G. VIGERS. 1986. Electron microscopy of frozen-hydrated biological material. *Nature* **319**: 631–636.
- STRICKLER, J. R. 1977. Observation of swimming performances of planktonic copepods. *Limnol. Oceanogr.* **22**: 165–170.
- TANKIN, R. S., AND R. FARHADIEH. 1971. Effects of thermal convection currents on formation of ice. *Int. J. Heat Mass Transfer.* **14**: 953–961.
- WIENS, J. A. 1989. Spatial scaling in ecology. *Funct. Ecol.* **3**: 385–397.

Received: 2 January 1997

Accepted: 13 October 1997

Amended: 7 November 1997